Supplementary Figure 1

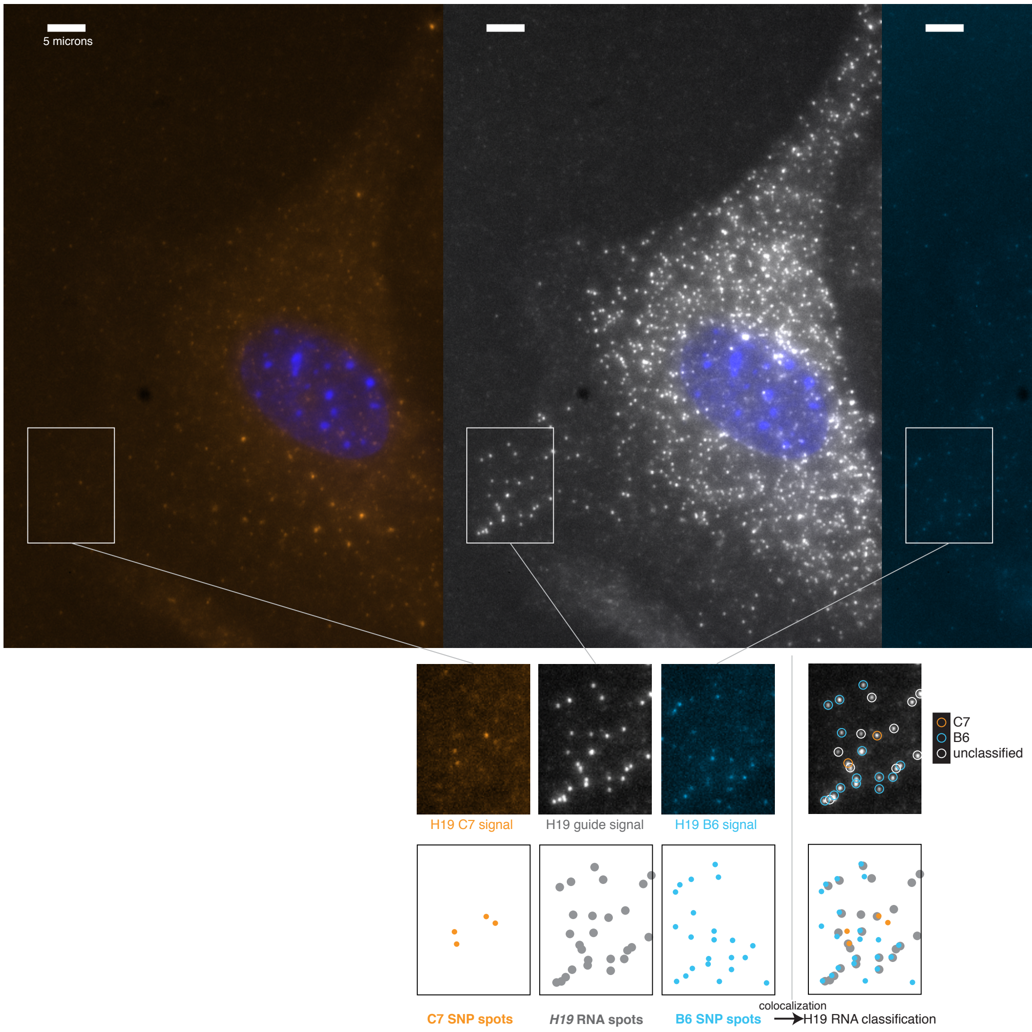

Supplementary Figure 1. Allele-specific expression in wild-type MEFs. Micrographs demonstrating allele-specific detection of B6 and C7 alleles in a representative B6xC7 MEF with a genotype opposite from that found in Figure 1B. Demonstrated from left to right in the three large micrographs as well as in a representative region below are *H19* C7 maternal probe, guide probe, and B6 paternal probe. The representative region shows how colocalization enables RNA classification. Under each micrograph are the computationally detected spots corresponding to single RNA transcripts. We labeled the guide probes with Cal Fluor 610, and C7 and B6-specific SNP FISH probes targeting the 5 SNPs between the two alleles with Cy5, Cy3, respectively. All scale bars correspond to 5 μm.

Supplementary Figure 2

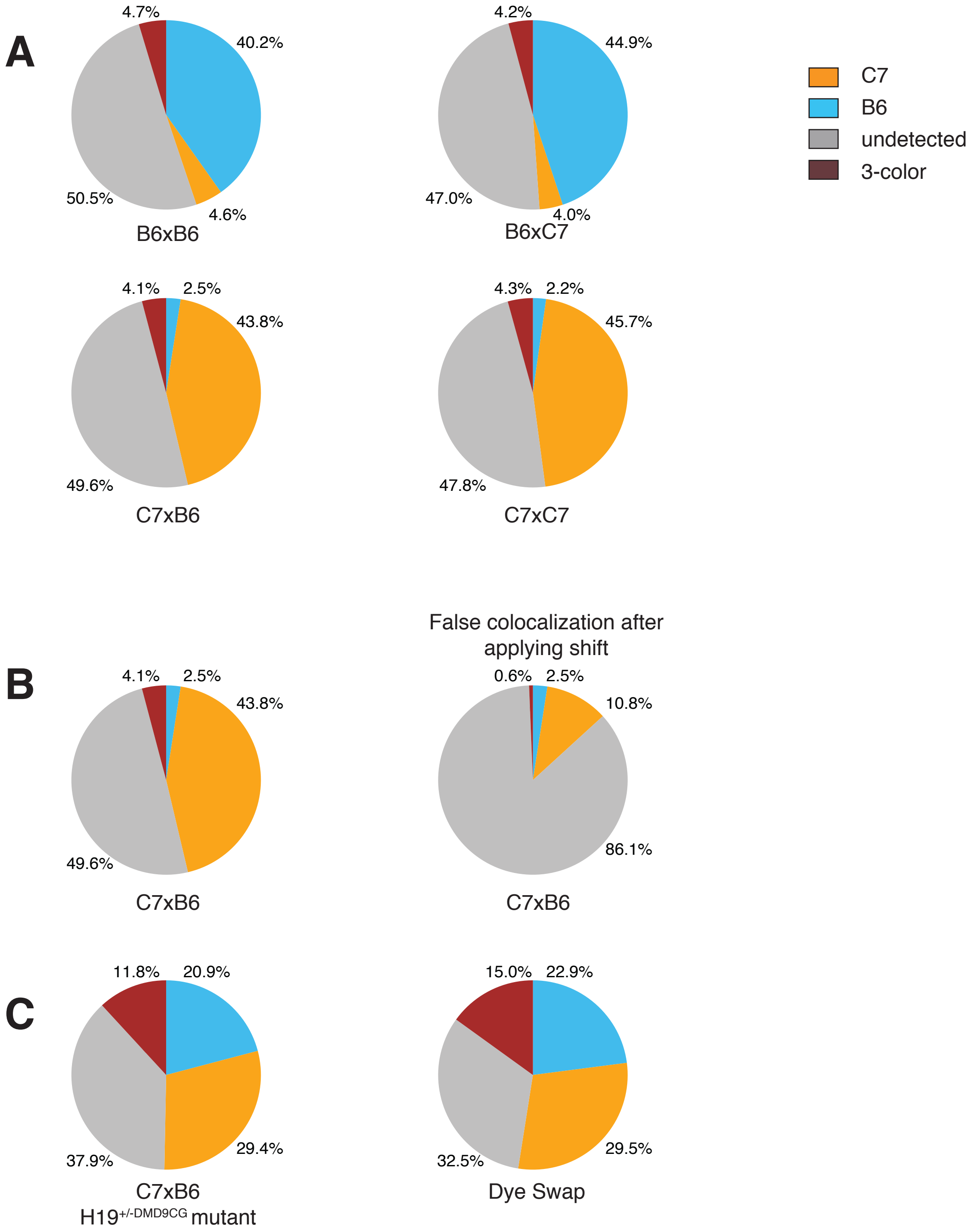

Supplementary Figure 2. Allele-specific expression detection is not affected by fluorophore and pixel colocalization. A. Efficiency of *H19* mRNA identification (B6, C7, neither or both) for wild-type MEFs of 4 different genotypes. B. Pixel shift demonstrates loss of colocalization of probes in C7xB6 wild-type MEFs. C. Overall expression of *H19* in MEFs from the C7xB6 $H19^{+/DMD\text{-}9CG}$ mutant mouse compared with overall expression with swapped fluorophores, which shows comparable ratios independent of dye effects.

Supplementary Figure 3

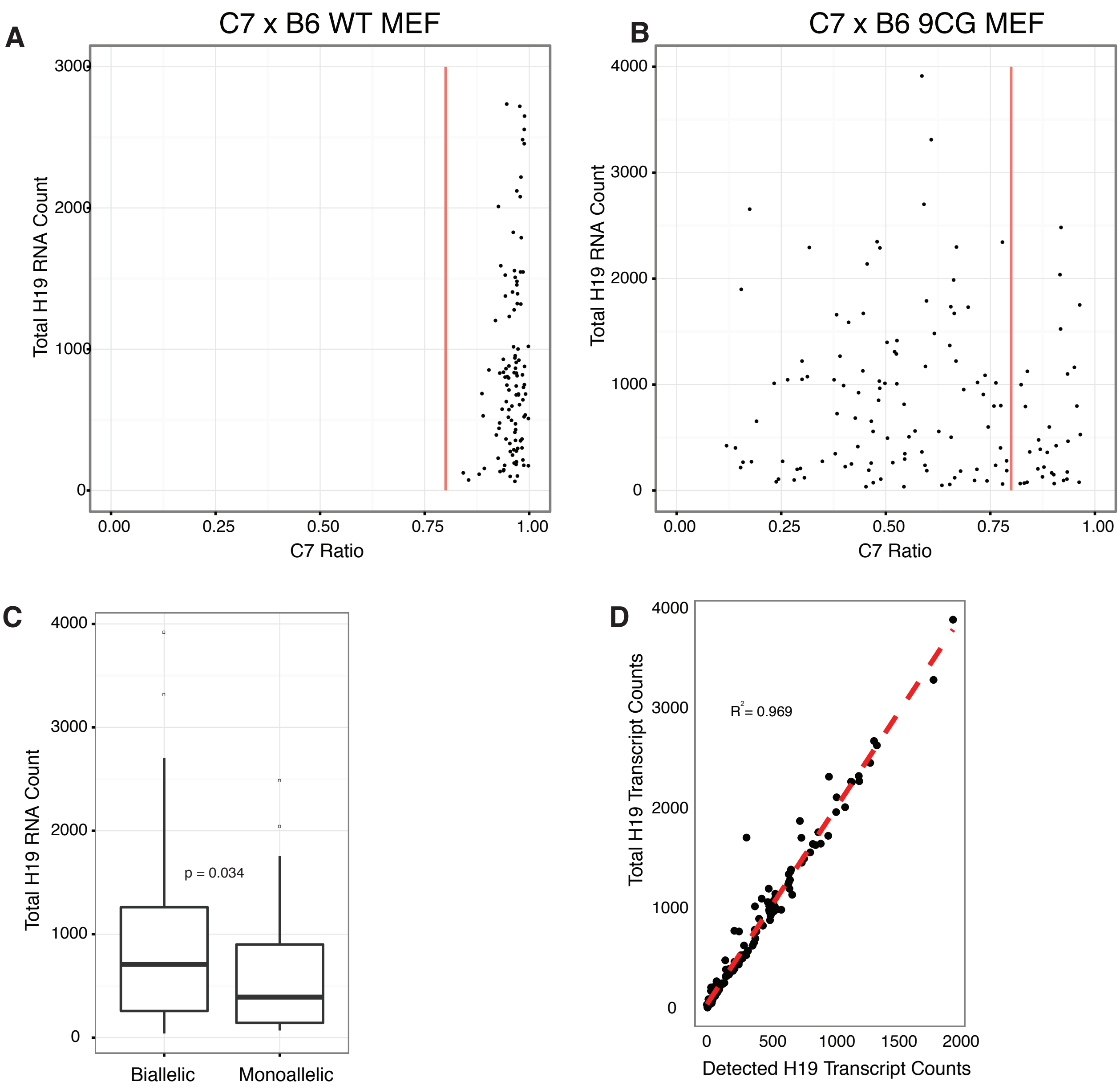

Supplementary Figure 3. Determination of monoallelic and biallelic ratios in wild-type and mutant MEFs. A. Scatter plot of allele-specific expression of C7xB6 wild-type MEFs. Almost all cells have a *H19* C7/total *H19* expression ratio greater than 0.8, suggesting 0.8 as an adequate cutoff for monoallelic *H19* expression. B. The *H19* C7 distribution and total *H19* RNA expression for C7xB6 *H19*$^{+/DMD\text{-}9CG}$ mutant MEFs. We classified cells with an *H19* C7/ total *H19* expression ratio greater 0.8 as monoallelic. C. Box plot showing *H19* RNA count distributions between monoallelic and biallelic cells in C7xB6 *H19*$^{+/DMD\text{-}9CG}$ mutant MEFs. Biallelic cells express approximately 50% more RNA on average than monoallelic cells (biallelic n = 102, monoallelic n = 31, p = 0.034 by bootstrapping through cell label permutation). D. Scatterplot showing linear relationship between detected *H19* transcript counts and total *H19* transcript counts in C7xB6 *H19*$^{+/DMD\text{-}9CG}$ mutant MEFs.

Supplementary Figure 4

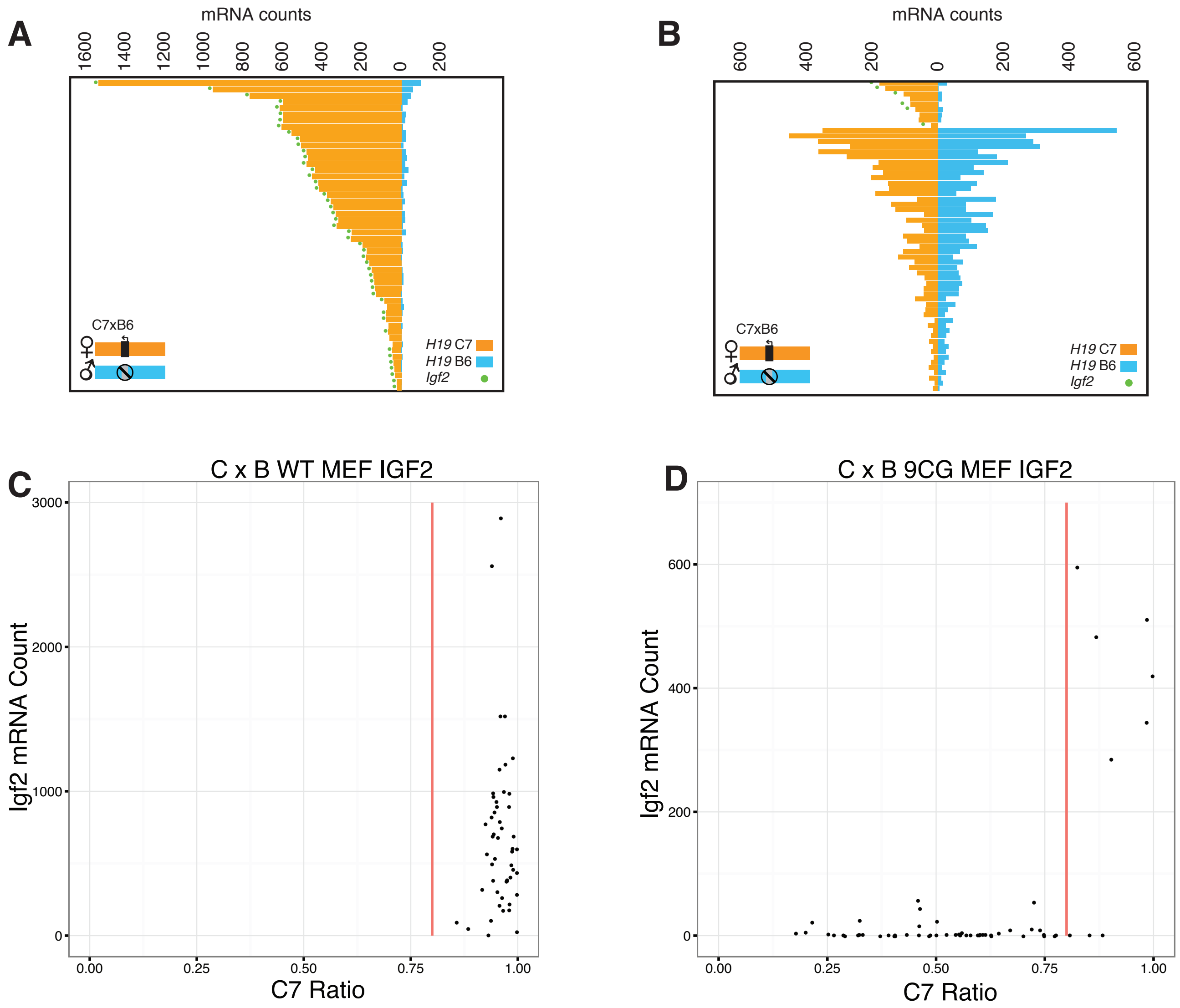

Supplementary Figure 4. *Igf2* expression in monoallelic and biallelic MEFs. A. *Igf2* expression (green dots) and *H19* expression (horizontal bars) in C7xB6 wild-type MEFs. B. *Igf2* expression (green dots) and *H19* expression (horizontal bars) in C7xB6 *H19*$^{+/DMD\text{-}9CG}$ mutant MEFs. C. Scatter-plot showing *H19* C7 expression bias versus total *Igf2* expression. Most cells have a C7/total *H19* expression ratio greater than 0.8, suggesting 0.8 as the cutoff for monoallelic *H19* expression. D. The *H19* C7 distribution and total *Igf2* RNA expression for C7xB6 *H19*$^{+/DMD\text{-}9CG}$ mutant MEFs. Only monoallelic cells express *Igf2* but not all monoallelic cells express *Igf2*.

Supplementary Figure 5

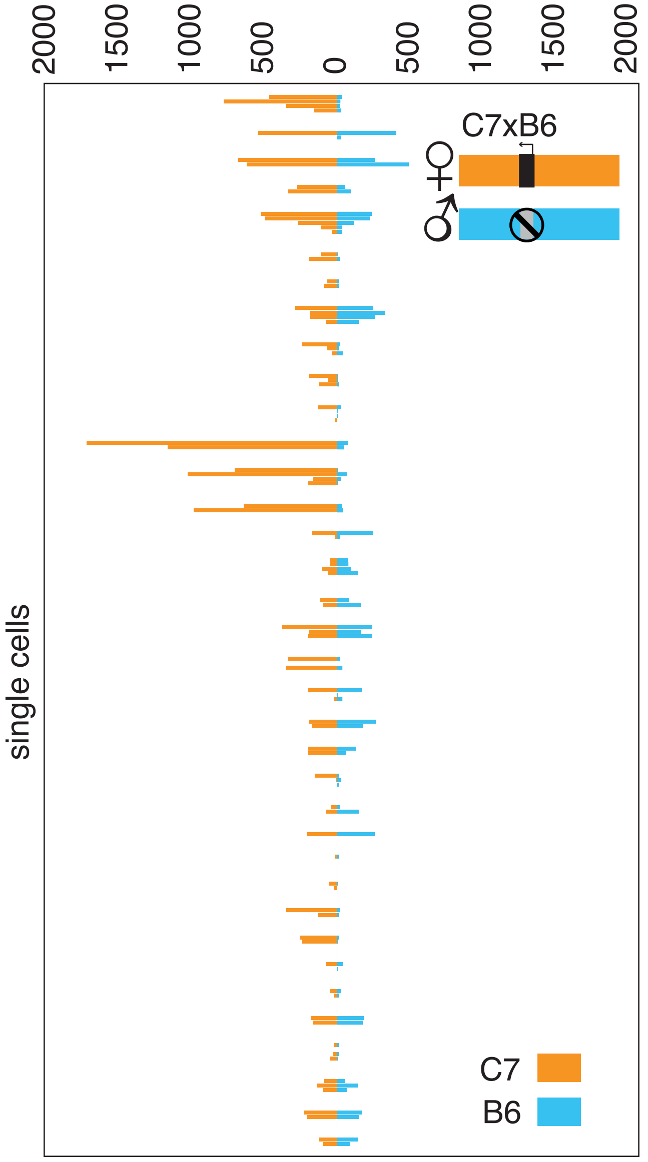

Supplementary Figure 5. MEF clones demonstrate that monoalleic and biallelic *H19* expression is heritable across cell divisions. C7xB6 *H19*$^{+/DMD-9CG}$ mutant MEF colonies from a second independent experiment (larger replicate of experiment in Fig. 3B).

Supplementary Figure 6

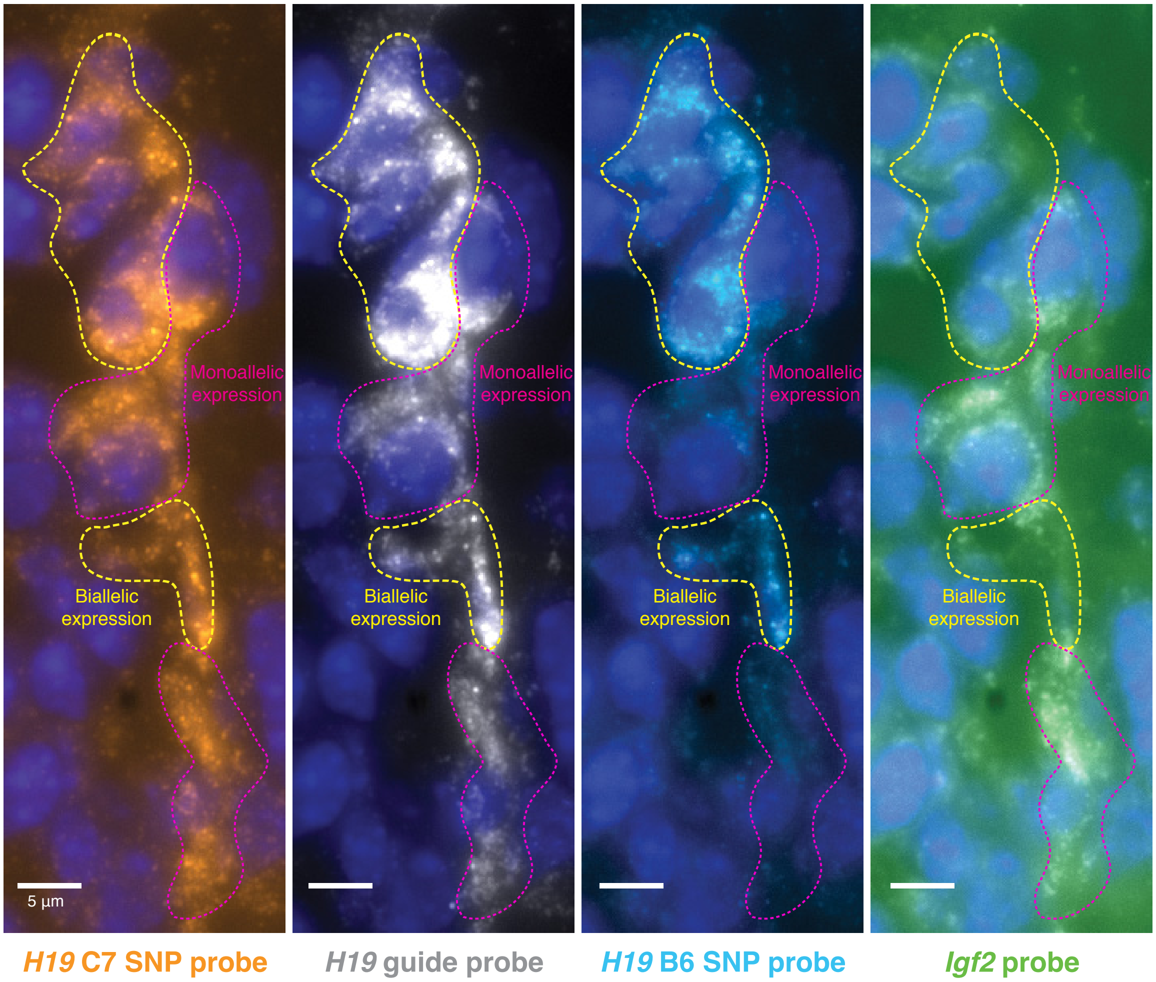

Supplementary Figure 6. Allele-specific expression in cardiac tissue from *H19*$^{+/DMD\text{-}9CG}$ mice with *Igf2* coexpression. Regions of monoallelic *H19* expression (magenta) and biallelic *H19* expression (yellow). *Igf2* (green) expresses only in regions of monoallelic *H19* expression.